***New Phytologist* Supporting Information Figs S1–S8, Tables S2–S4 & S6 and Notes S1 & S2**

Article title: **Adapting through glacial cycles: insights from a long-lived tree (*Taxus baccata* L.)**

Authors: Maria Mayol, Miquel Riba, Santiago C. González-Martínez, Francesca Bagnoli, Jacques-Louis de Beaulieu, Elisa Berganzo, Concetta Burgarella, Marta Dubreuil, Diana Krajmerová, Ladislav Paule, Ivana Romšáková, Cristina Vettori, Lucie Vincenot, Giovanni G. Vendramin

Article acceptance date: 01 May 2015

The following Supporting Information is available for this article:

Fig. S1 Geographical location of the twelve different sets of populations used in ABC simulations. Maps 1-10 correspond to simulations performed considering two gene pools (*Western*, *Eastern*). Maps 11-12 correspond to simulations performed considering three gene pools (*Western*, *Eastern*, *Iran*). The upper left number in each map indicates the number of the simulation.

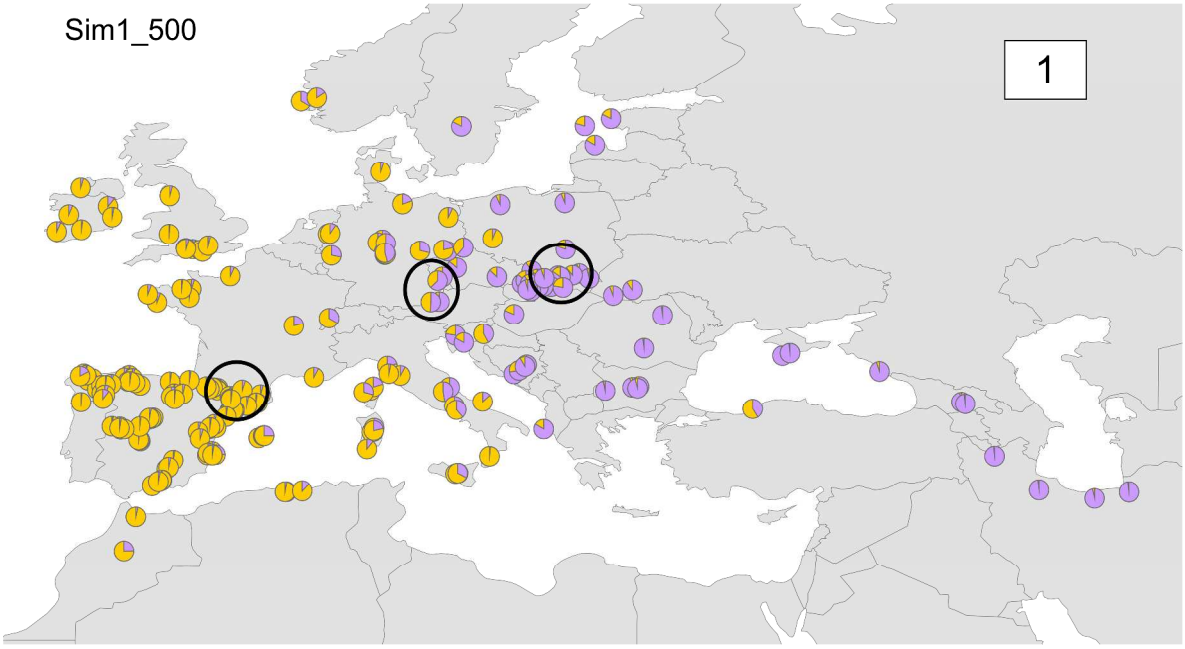

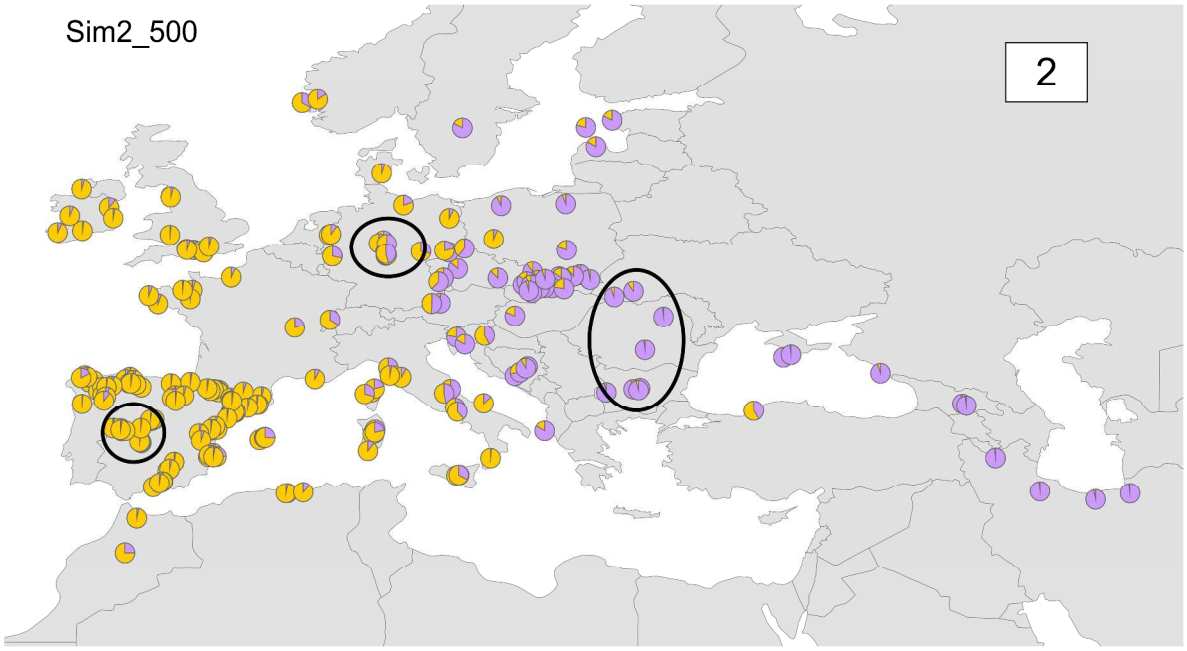
Sim2_500
2

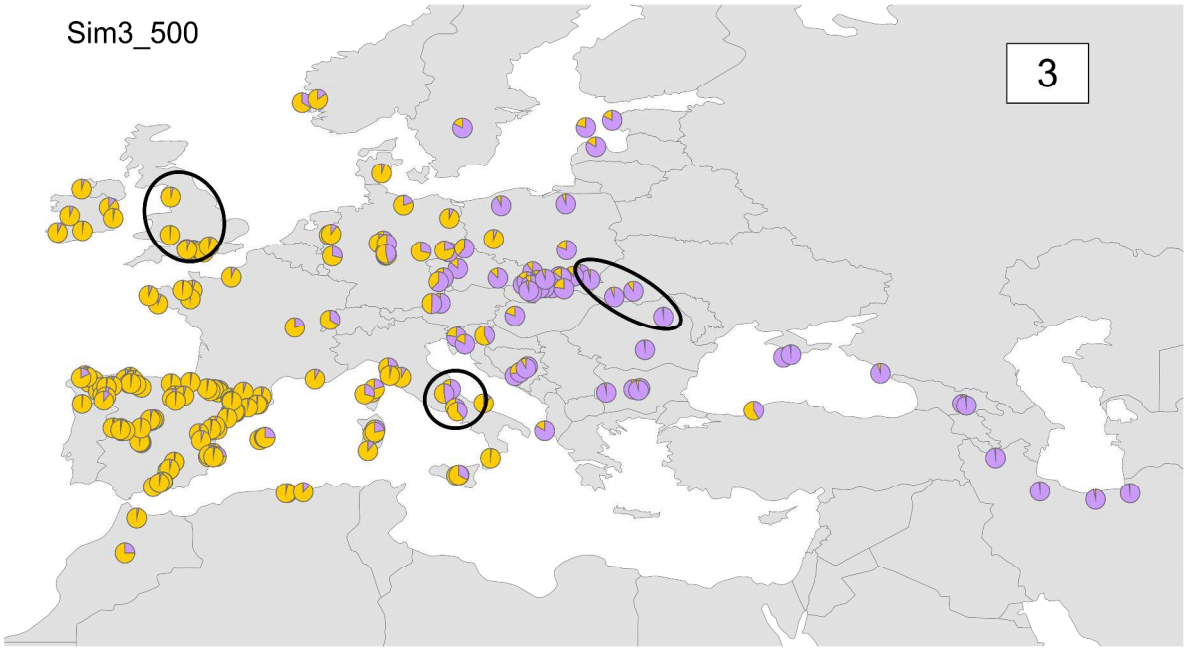
Sim3_500
3

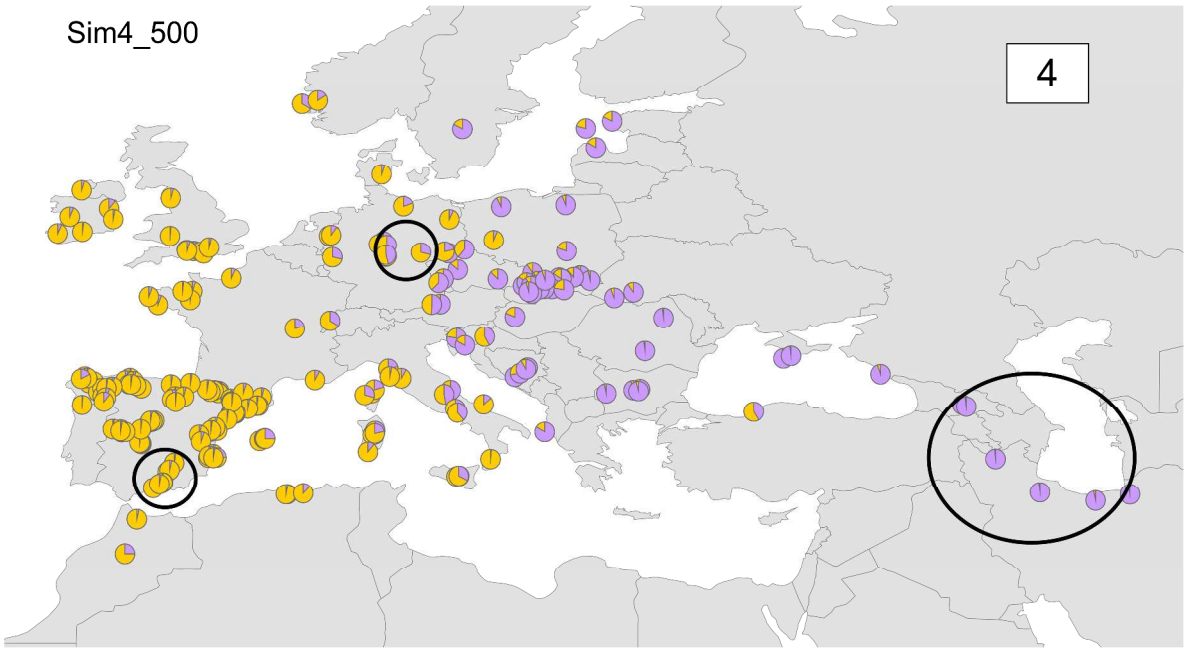
Sim4_500
4

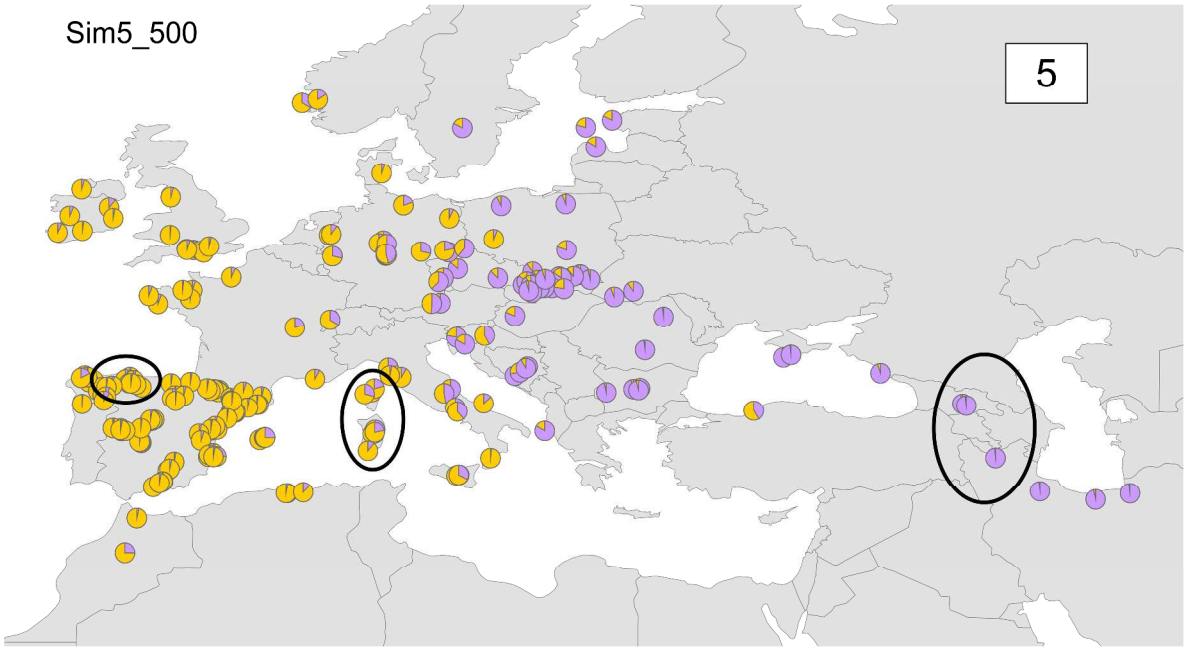
Sim5_500
5

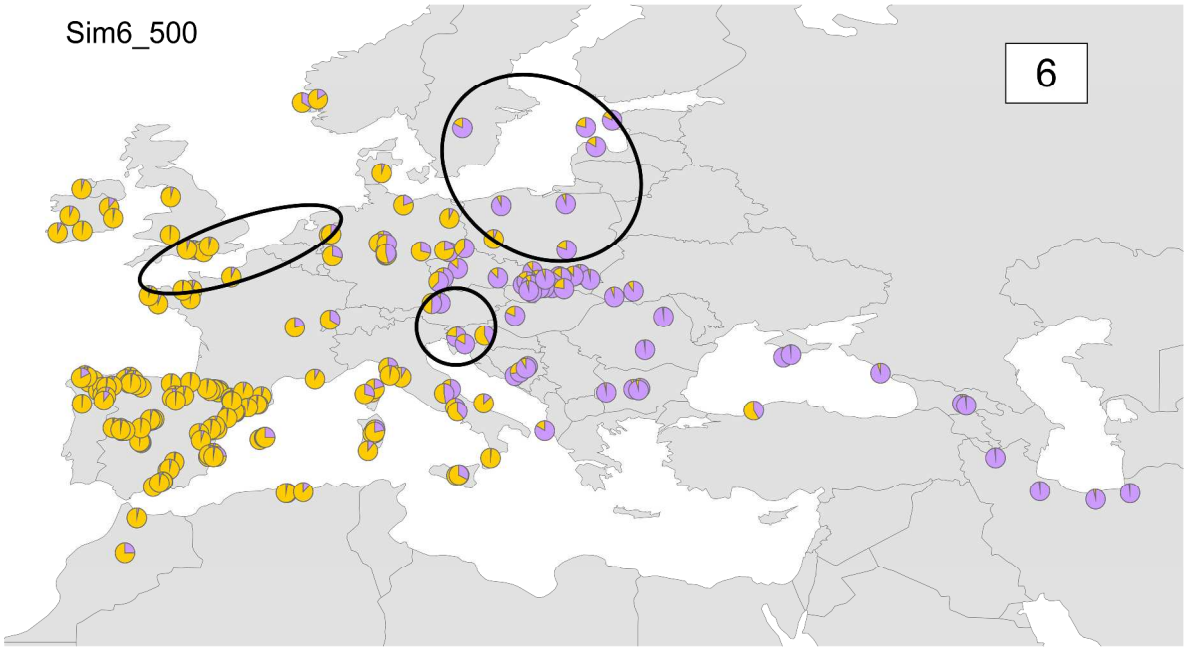
Sim6_500
6

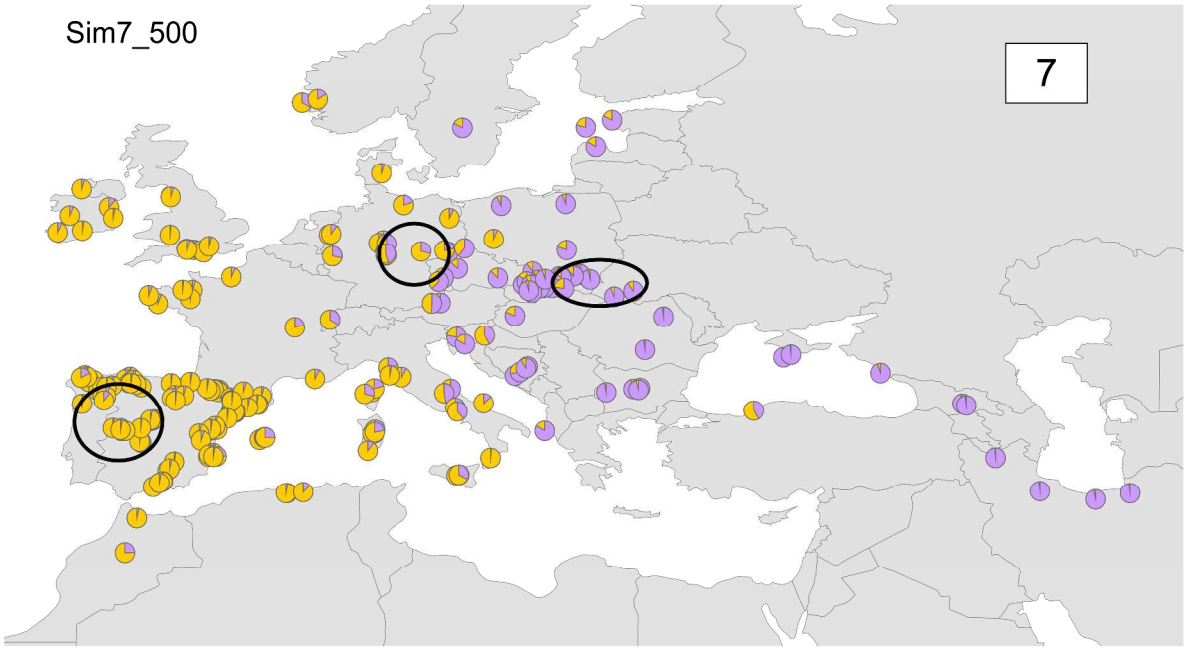
Sim7_500
7

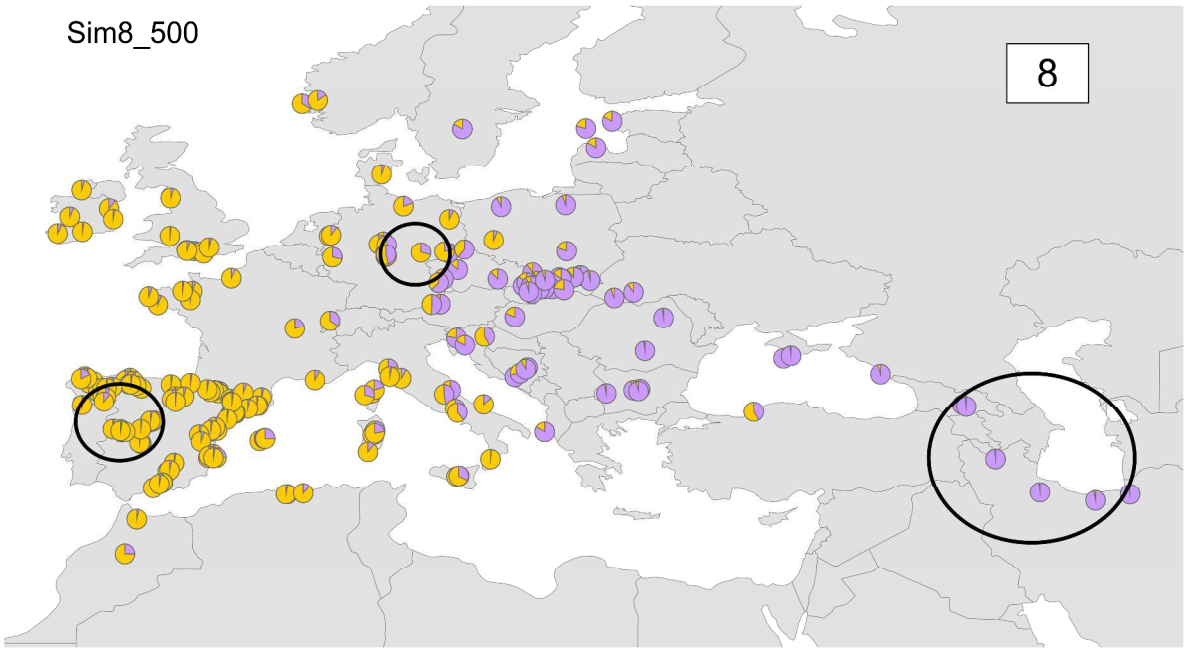
Sim8_500
8

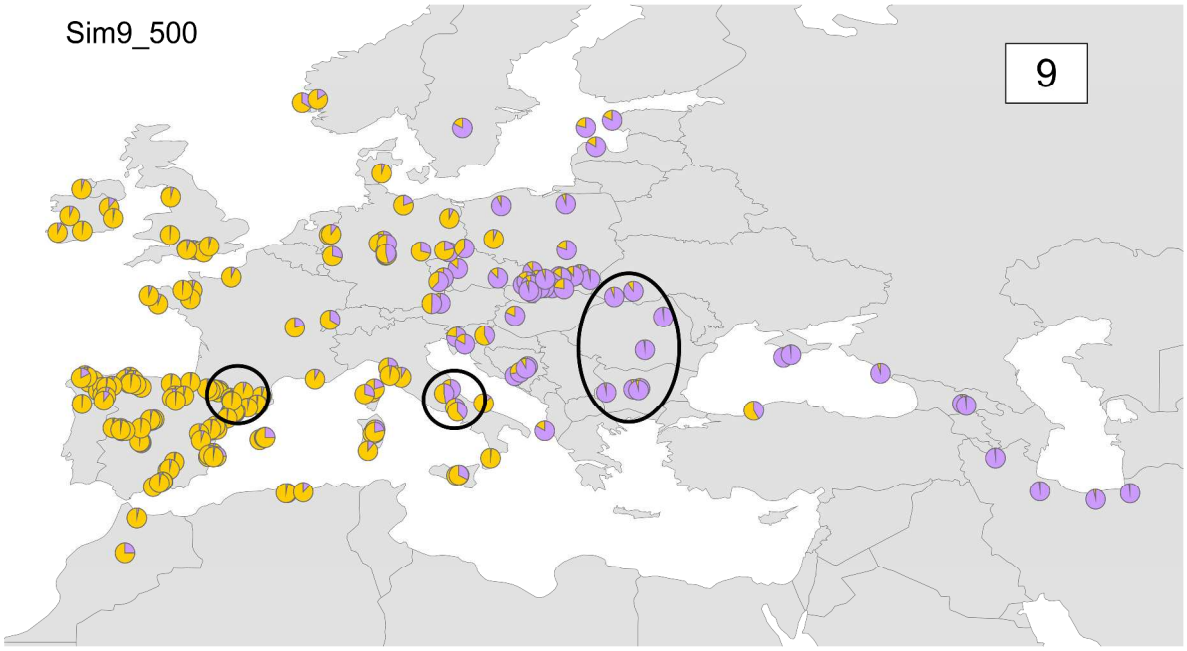
Sim9_500
9

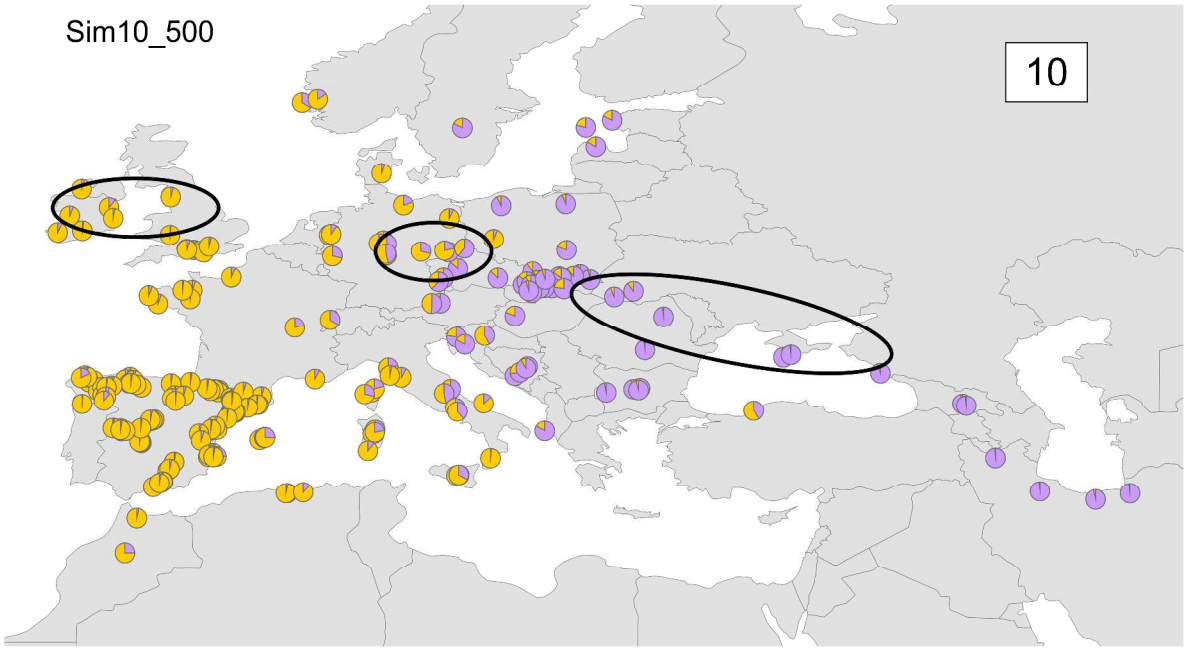
Sim10_500
10

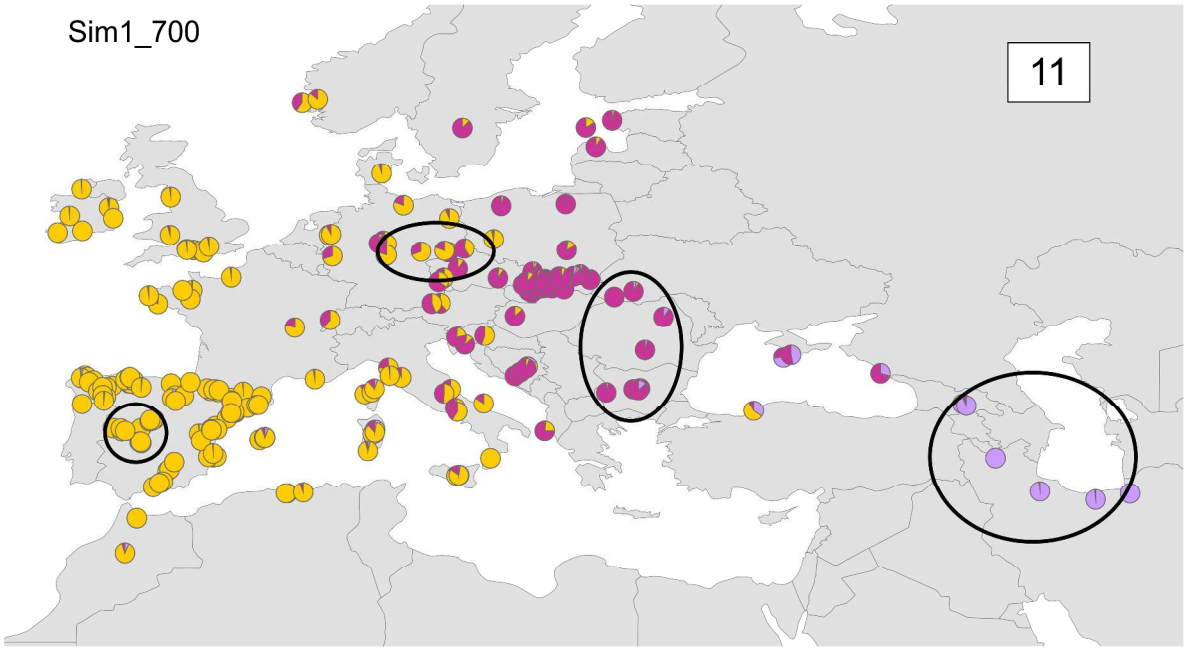
Sim1_700
11

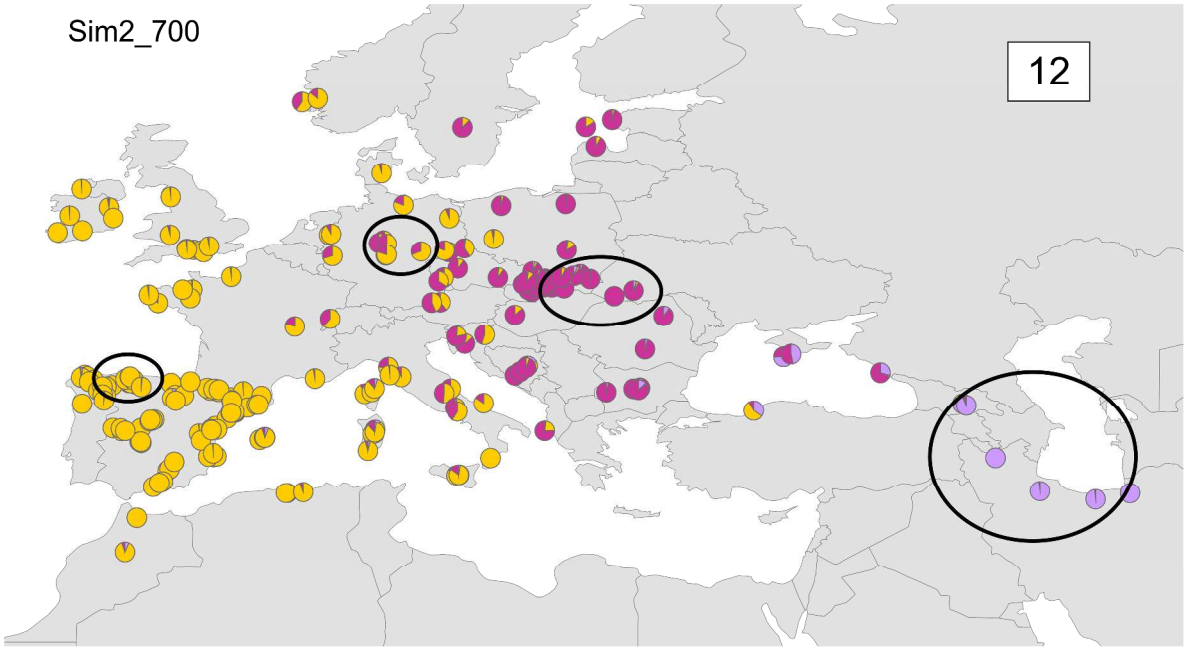

Fig. S2 Pre-evaluation of scenarios and prior distributions. Principal Component Analysis was performed in the space of summary statistics on 50,000 simulated data sets. The observed data set (large yellow dot) is positioned well within the cloud of simulated data sets (small dots).

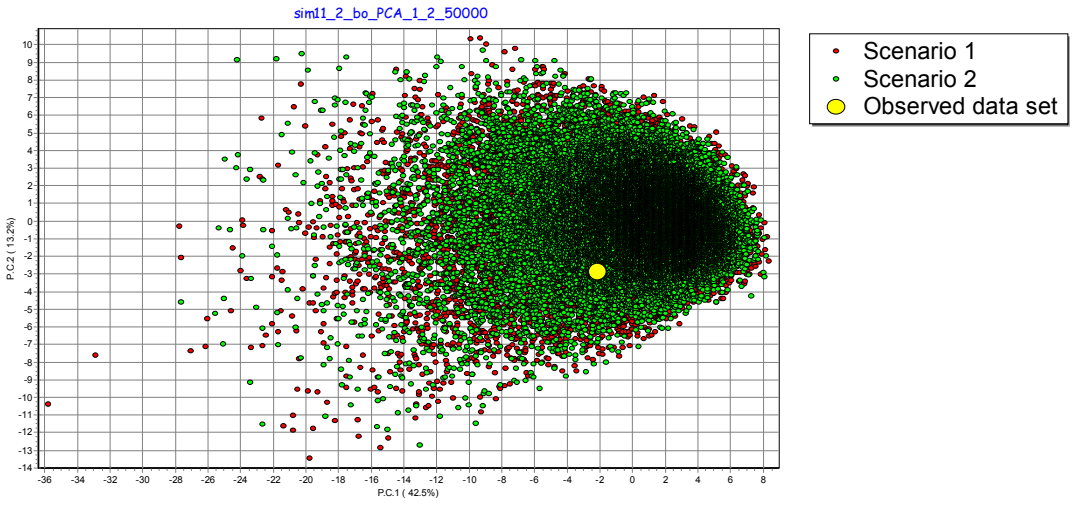

Fig. S3 Geographical distribution of the two chloroplast haplotypes detected in the *trnS–trnQ* and *trnL–trnF* intergenic spacers. In each map, the green and red circles indicate the different haplotypes.

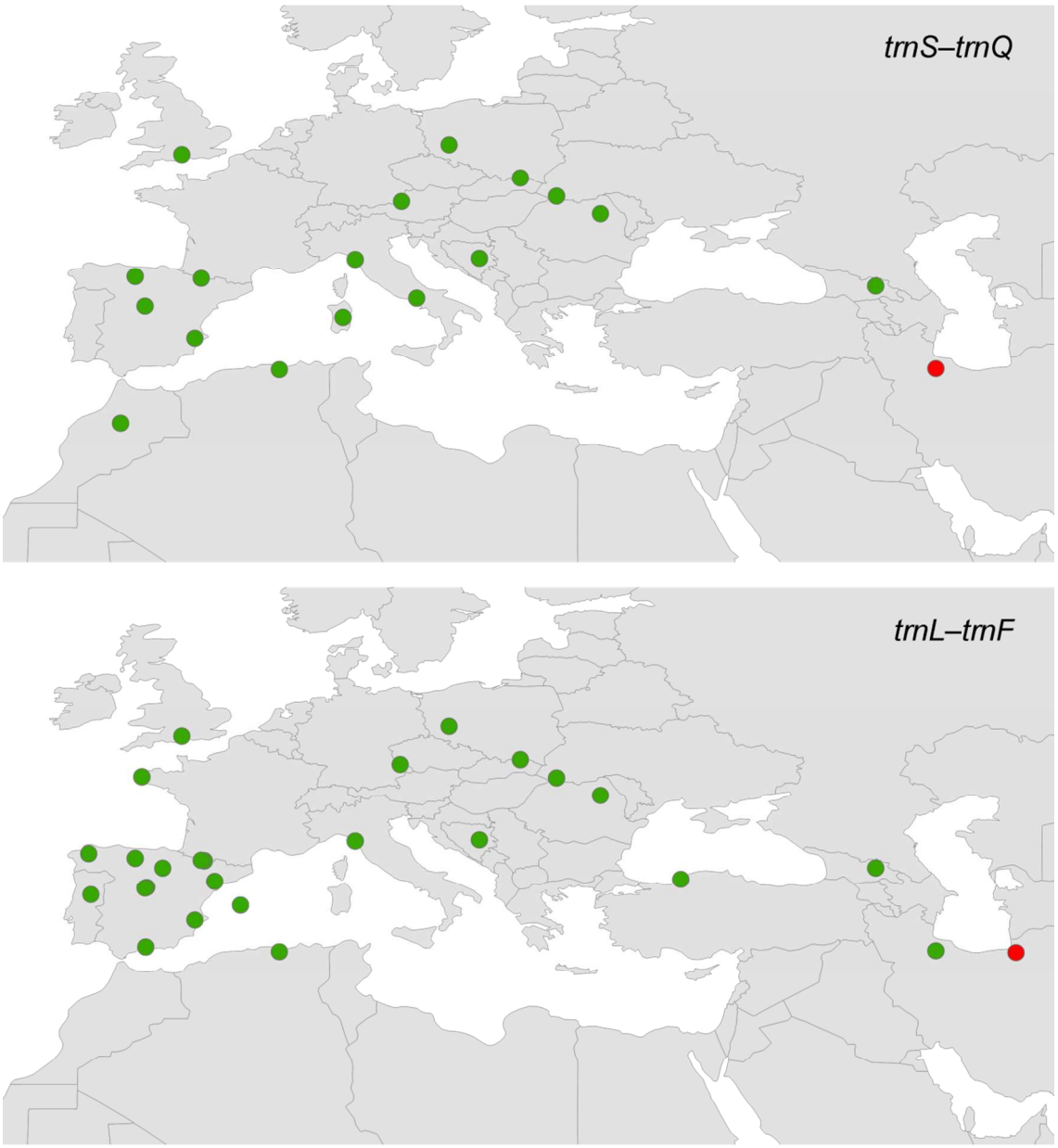

Fig. S4 Summary of the clustering results using TESS for *K*=2, and STRUCTURE for *K*=3 and *K*=4. Pie charts are averaged values of the different runs for the proportion of membership to each genetic cluster.

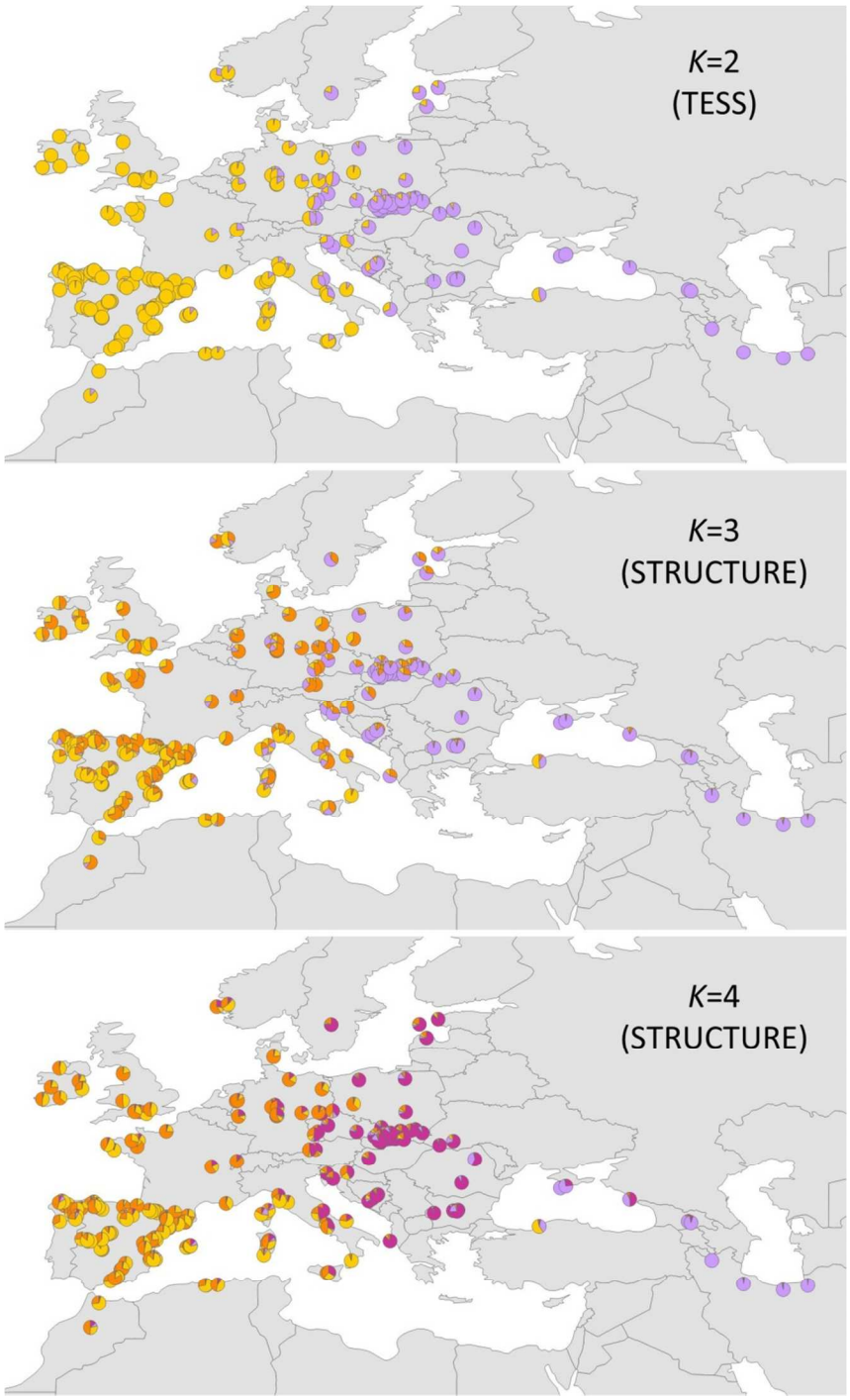

Fig. S5 Prior (red) and posterior (green) distributions of estimated parameters for simulation sim2_700 under Scenario C in Fig. 2. N1=current effective population size of the *Iran* gene pool; N2=current effective population size of the *Eastern* gene pool; N3=current effective population size of the *Admixed* samples; N4=current effective population size of the *Western* gene pool.

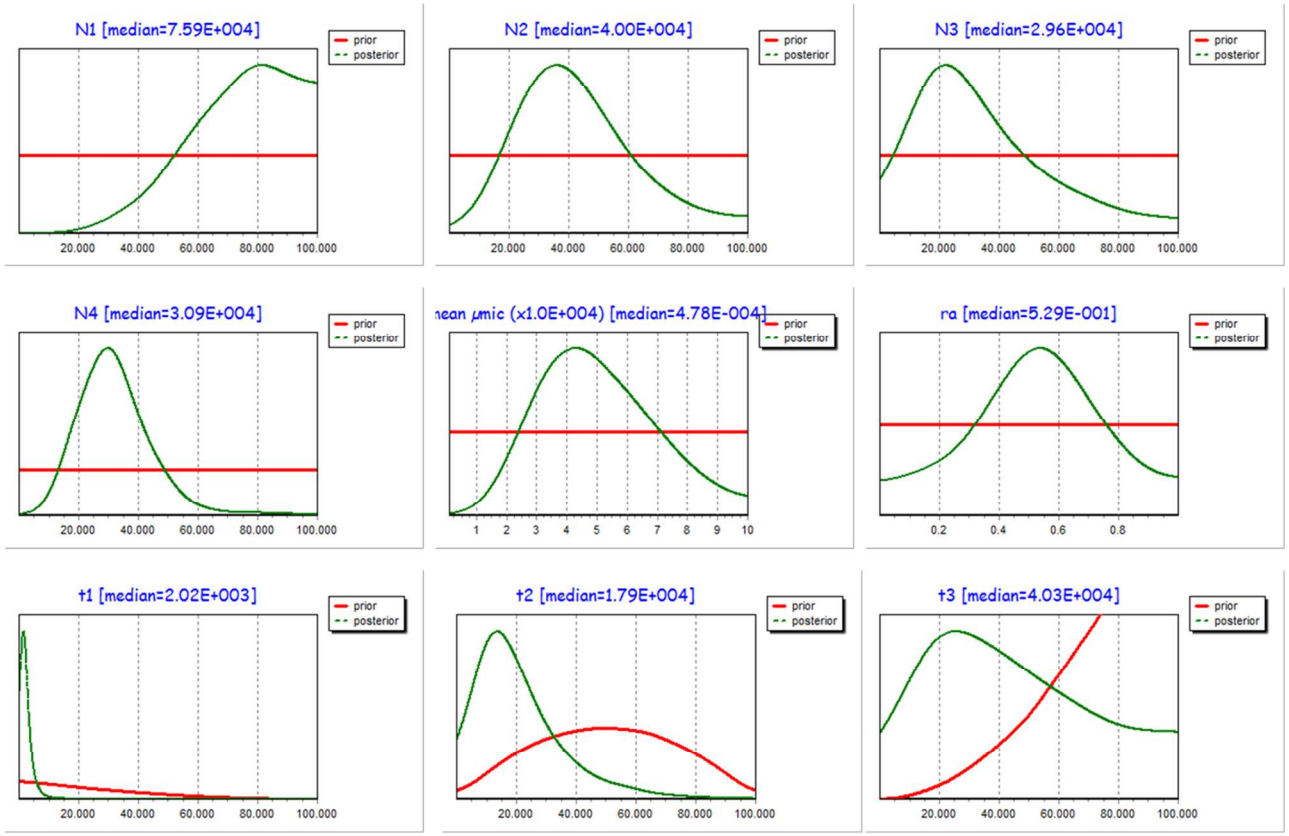

Fig. S6 Principal Component Analysis plot of environmental variables for the present time described in Table S4. Axes 1 and 2 explain 52% of the variation for the present climate. Note that populations from *Western* (orange squares) and *Eastern* (lilac circles) gene pools are separated along the PC1 axis. Populations of *Admixed* composition are depicted as green triangles.

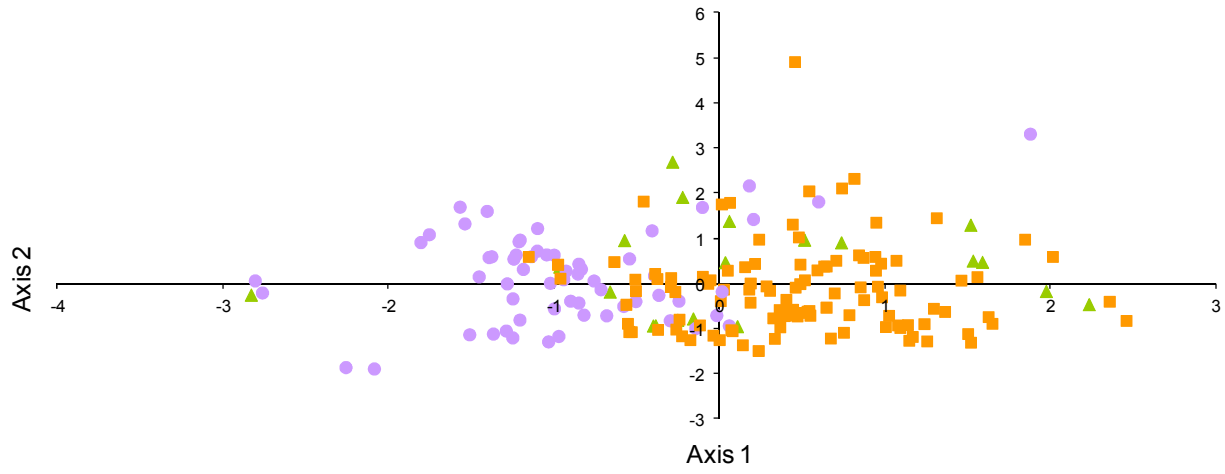

Fig. S7 MAXENT predicted suitability for *Taxus baccata* based on climatic variables at three time periods: LIG=Last interglacial (~120,000-140,000 yrs BP), LGM-CCSM and LGM-MIROC=Last Glacial Maximum (~21,000 yrs BP), PRE=present conditions (~1950-2000). The models were produced using the whole dataset (238 occurrence points). Darker colours indicate higher probabilities of suitable climatic conditions. Not suitable areas and those with logistic output values below the maximum training sensitivity plus specificity (MTSS) threshold indicated in grey.

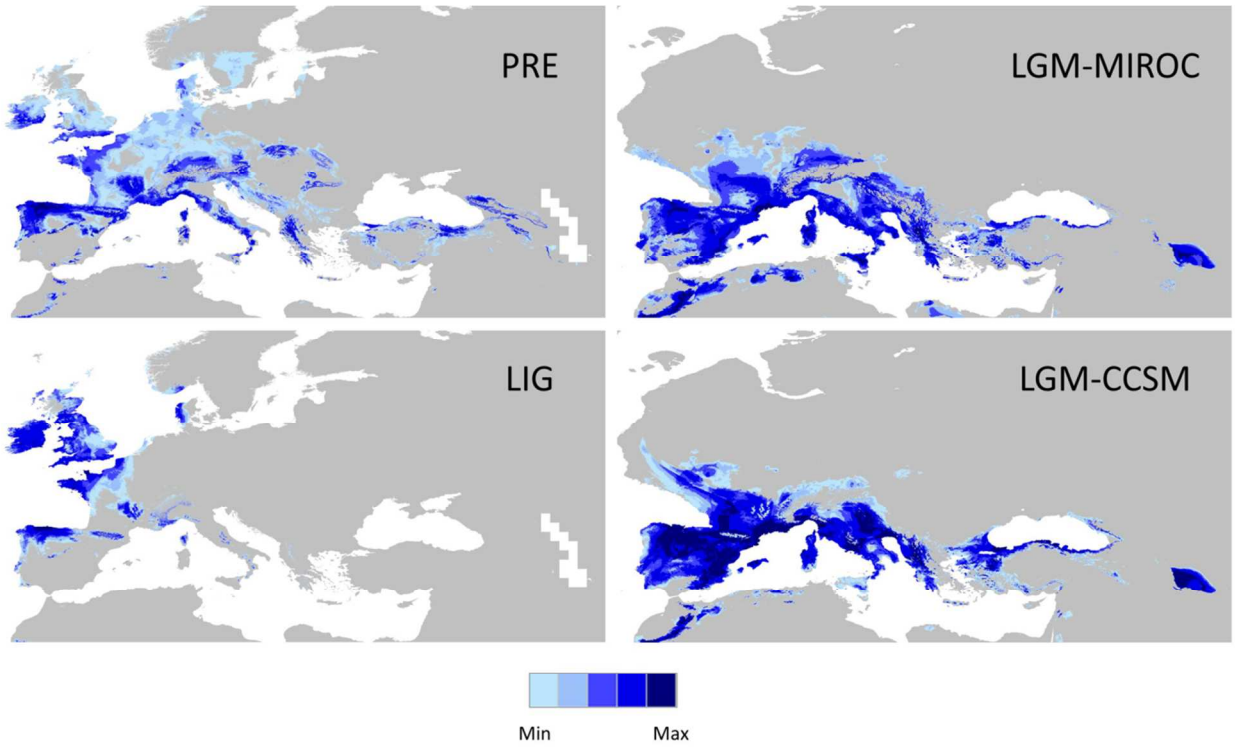

Fig. S8 Relationship between sex-ratio and temperature. Populations (*N*=92) are distributed along the Western Mediterranean and the British Isles (*Western* gene pool) and Central and Northern Europe (*Eastern* gene pool). Note that populations of the western group have similar sex ratio trends to those of the eastern populations but at higher temperatures.

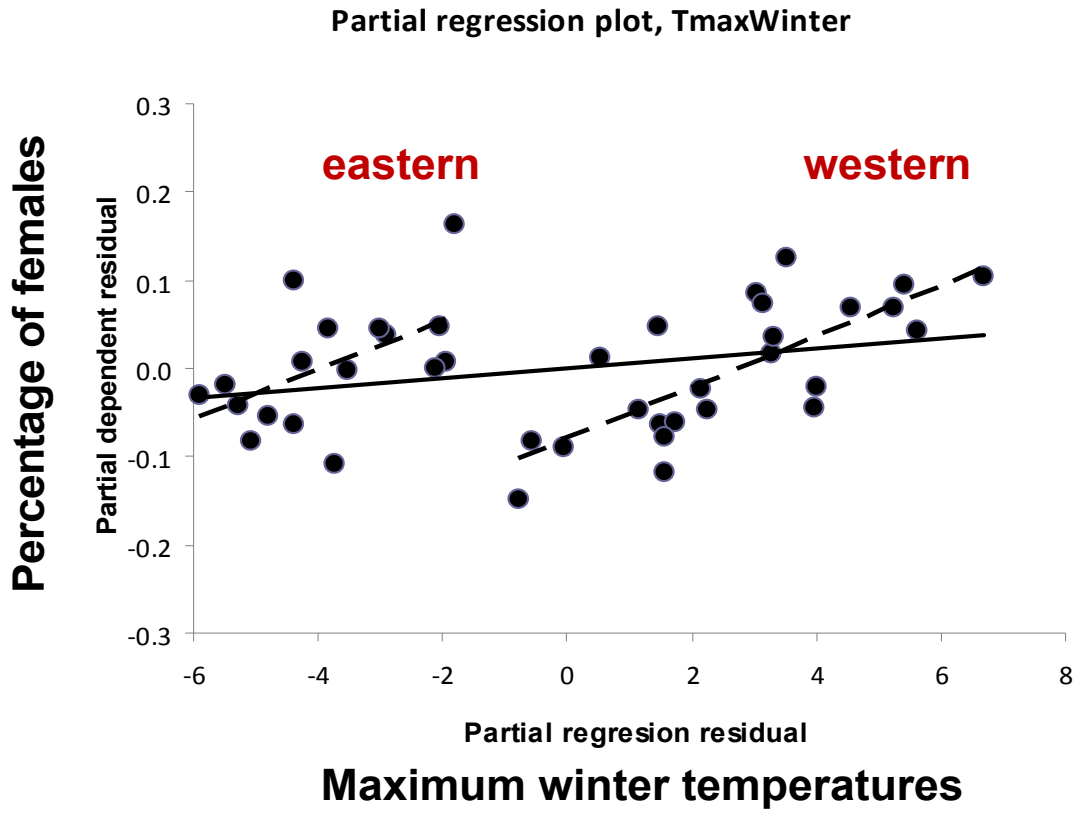

Table S2 Sampled populations and polymorphic sites for the *trnS–trnQ* intergenic spacer.

Country	Population	Polymorphic sites		
		398	502	521
Algeria	Algeria*	T	A	T
Austria	Austria*	T	A	T
Bosnia-Herzegovina	Ajdonovici	T	A	T
Georgia	Batsara	T	A	T
Italy	Apulia*	T	A	T
Italy	Lazio*	T	A	T
Italy	Sardinia*	T	A	T
Iran	Guilan Province	G	G	G
Morocco	Morocco*	T	A	T
Poland	Góra Ślaska	T	A	T
Spain	Tosande	T	A	T
Spain	Bujaruelo	T	A	T
Spain	Font Roja	T	A	T
Spain	Rascafría	T	A	T
Romania	Tudora	T	A	T
Slovakia	Becherovská	T	A	T
Ukraine	Ugolka	T	A	T
United Kingdom	Wales*	T	A	T

*Retrieved from GenBank (Schirone et al. 2010)

Table S3 Sampled populations and polymorphic sites for the *trnL–trnF* intergenic spacer.

Country	Population	Polymorphic sites	
		87	272
Algeria	Chréa	T	-
Bosnia-Herzegovina	Ajdonovici	T	-
Czech Republic	Železná ruda	T	-
France	Forêt du Cranou	T	-
Georgia	Batsara	T	-
Iran	Guilan Province	T	-
Iran	Golestan Province-1	G	A
Iran	Golestan Province-2	G	A
Italy	Italy*	T	-
Poland	Góra Ślaska	T	-
Portugal	Portugal*	T	-
Romania	Tudora	T	-
Slovakia	Becherovská	T	-
Spain	Canencia*	T	-
Spain	Pineta	T	-
Spain	Mallorca (Planicia-1)	T	-
Spain	Mallorca (Planicia-2)	T	-
Spain	Galicia	T	-
Spain	Taverna-1	T	-
Spain	Taverna-2	T	-
Spain	Sierra Tejeda-1	T	-
Spain	Sierra Tejeda-2	T	-
Spain	Bujaruelo	T	-
Spain	Tosande	T	-
Spain	Rascafría-1	T	-
Spain	Rascafría-2	T	-
Spain	Sorzano (Logroño)	T	-
Spain	Font Roja	T	-
Turkey	Turkey*	T	-
Ukraine	Ugolka	T	-
United Kingdom	Scotland*	T	-

* Retrieved from GenBank (Shah et al. 2008)

Table S4 Bioclimatic variables and standardized loadings for the two first axes of the PCA analysis (present climate). In bold, variables with loadings higher than 0.5. Mean diurnal range = Mean of monthly (max temp - min temp).

Variable	Description	First axis (PC1)	Second axis (PC2)
BIO1	Annual mean temperature	**0.96**	-0.07
BIO2	Mean diurnal range	-0.09	-0.18
BIO4	Temperature seasonality	**-0.55**	-0.17
BIO5	Max temperature of the warmest month	**0.57**	-0.20
BIO6	Min temperature of the coldest month	**0.95**	0.03
BIO8	Mean temperature of the wettest quarter	-0.01	-0.22
BIO9	Mean temperature of the driest quarter	**0.64**	0.04
BIO10	Mean temperature of the warmest quarter	**0.76**	-0.17
BIO11	Mean temperature of the coldest quarter	**0.97**	0
BIO12	Annual precipitation	-0.05	**0.87**
BIO13	Precipitation of the wettest month	-0.10	**0.98**
BIO14	Precipitation of the driest month	-0.23	0.39
BIO15	Precipitation seasonality	0.01	0.12
BIO16	Precipitation of the wettest quarter	-0.08	**0.99**
BIO17	Precipitation of the driest quarter	-0.14	0.41
BIO18	Precipitation of the warmest quarter	**-0.50**	0.39
BIO19	Precipitation of the coldest quarter	0.25	**0.78**

Table S6 Analysis of molecular variance (AMOVA). (a) Assuming no regional differentiation. (b) Populations grouped in two genetic clusters: *Western-Eastern*.

Source of variation	df	Sum of squares	Variance components	Percentage of variation
(a)				
Among populations	194	4554.81	0.43021	16.41*
Within populations	9463	20742.28	2.19193	83.59
(b)				
Among *W-E* genetic clusters	1	781.52	0.18685	6.85*
Among populations within clusters	172	3453.83	0.35719	13.09*
Within population	8562	18702.23	2.18433	80.06*

* $P < 0.001$ (significant after 10,000 permutations).

Notes S1 Details and results of model checking and confidence in scenario choice.

Scenario choice. The power of the model choice procedure was evaluated by estimating type I and type II errors from 500 pseudo-observed data sets simulated under each competing scenario, as described in Cornuet *et al*. (2010). Type I error was estimated as the proportion of data sets simulated under the best supported scenario in each simulation that resulted in a highest posterior probability for the alternative scenario. Type II error was estimated by the proportion of data sets that resulted in highest posterior probability of the best supported scenario, although simulated with the other one. Consequently, type I error for the best supported scenario in each simulation is identical to type II error for the alternative scenario and viceversa. In a first test, the scenario with the highest posterior probability was recorded irrespective of the value of the posterior probability. Additionally, in a second test, we computed type I and II errors but taken into account only those simulations with a posterior probability (*PP*) equal or superior to that of the best scenario ($PP \geq 0.8$).

Estimates of type I and II errors for the first test, i.e. when considering all scenarios irrespective of their posterior probability, were between 15-20% (Table 1), indicating ~80% statistical power. This power increased significantly in the second test, i.e. when we only considered simulations with $PP \geq 0.8$, reaching about 94-98% statistical power (Table 1). Altogether, our power tests indicated that only at a low values of posterior probability competing scenarios were misclassified. Therefore, the evaluation of the performance of the model choice procedure clearly showed that the method had high power to distinguish between the alternative demographic scenarios that we investigated with our data set.

Model checking. The goodness-of-fit of our model was assessed by simulating 1,000 data sets under each scenario using parameter values drawn from their posterior distributions. In order to avoid overestimating the fit of the scenario, the similarity between simulated and real data sets was estimated using three summary statistics (*S*) differing from the summary statistics used to conduct model choice: mean allele size variance for each cluster and between pairs of clusters, and $(\delta\mu)^2$ distance between pairs of clusters. The discrepancy between simulated and observed data was then assessed by comparing the observed value with the values obtained from the

simulations, and computing a *P*-value as Prob ($S_{simulated} < S_{observed}$) and 1.0 - Prob ($S_{simulated} < S_{observed}$) for Prob ($S_{simulated} < S_{observed}$) $\leq$ 0.5 and > 0.5, respectively.

The number of observed summary statistics deviating significantly from its simulated distribution was low (Table 2). For "500-sample datasets" we found that, at most, one of the nine summary statistics deviated significantly from its simulated distribution, while for "700-sample datasets", none of 16 summary statistics lay outside the confidence intervals, confirming the compatibility of the model with the observed data .

Table 1 Type I and Type II error rates after 500 test data sets (i.e., pseudo-observed data sets). *PP* = posterior probability.

Simulation	Best supported scenario in the simulation (*PP*)	Type I error	Type II error	Type I error (*PP* ≥ 0.8)	Type I error (*PP* ≥ 0.8)
sim1_500	A (>0.9)	0.200	0.194	0.032	0.038
sim2_500	A (>0.9)	0.208	0.166	0.040	0.018
sim3_500	A (~0.6)	0.201	0.187	0.039	0.020
sim4_500	B (~0.6)	0.174	0.192	0.020	0.032
sim5_500	B (~0.7)	0.186	0.186	0.038	0.018
sim6_500	A (>0.9)	0.208	0.162	0.056	0.026
sim7_500	A (>0.9)	0.196	0.170	0.038	0.028
sim8_500	B (>0.9)	0.214	0.188	0.062	0.044
sim9_500	A (~0.8)	0.184	0.158	0.036	0.026
sim10_500	A (>0.9)	0.224	0.188	0.044	0.042
sim1_700	C (>0.9)	0.194	0.162	0.022	0.016
sim2_700	C(>0.9)	0.164	0.158	0.030	0.018

Table 2 Number of summary statistics that displayed outlying values compared with the observed ones in the model checking procedure. The probability ($S_{simulated} < S_{observed}$) given for each summary statistics (S) was computed from 1,000 data sets simulated from the posterior distributions of parameters obtained under a given scenario.

		Number of outlying summary statistics		
Simulation	Scenario	$P < 0.05$	$P < 0.01$	$P < 0.001$
sim1_500	A	1	0	0
sim2_500	A	1	0	0
sim3_500	A	1	0	0
sim4_500	B	0	0	0
sim5_500	B	0	0	0
sim6_500	A	1	0	0
sim7_500	A	0	0	0
sim8_500	B	0	0	0
sim9_500	A	1	0	0
sim10_500	A	0	0	0
sim1_700	C	0	0	0
sim2_700	C	0	0	0

Notes S2 Species distribution models and correlations between genetic distance (F_{ST}) and environmental variables obtained using the "BIOCLIM" algorithm implemented in DIVA-GIS v.7.5.

Fig. 1 BIOCLIM predicted suitability for *Taxus baccata* based on climatic variables at three time periods: LIG=Last interglacial (~120,000-140,000 yrs BP), LGM-CCSM and LGM-MIROC=Last Glacial Maximum (~21,000 yrs BP), PRE=present conditions (~1950-2000). The models were produced using the whole dataset (238 occurrence points). Darker colours indicate higher probabilities of suitable climatic conditions. Not suitable areas and those with medium or low suitability values (i.e., below the 5-95th percentile interval) are indicated in grey.

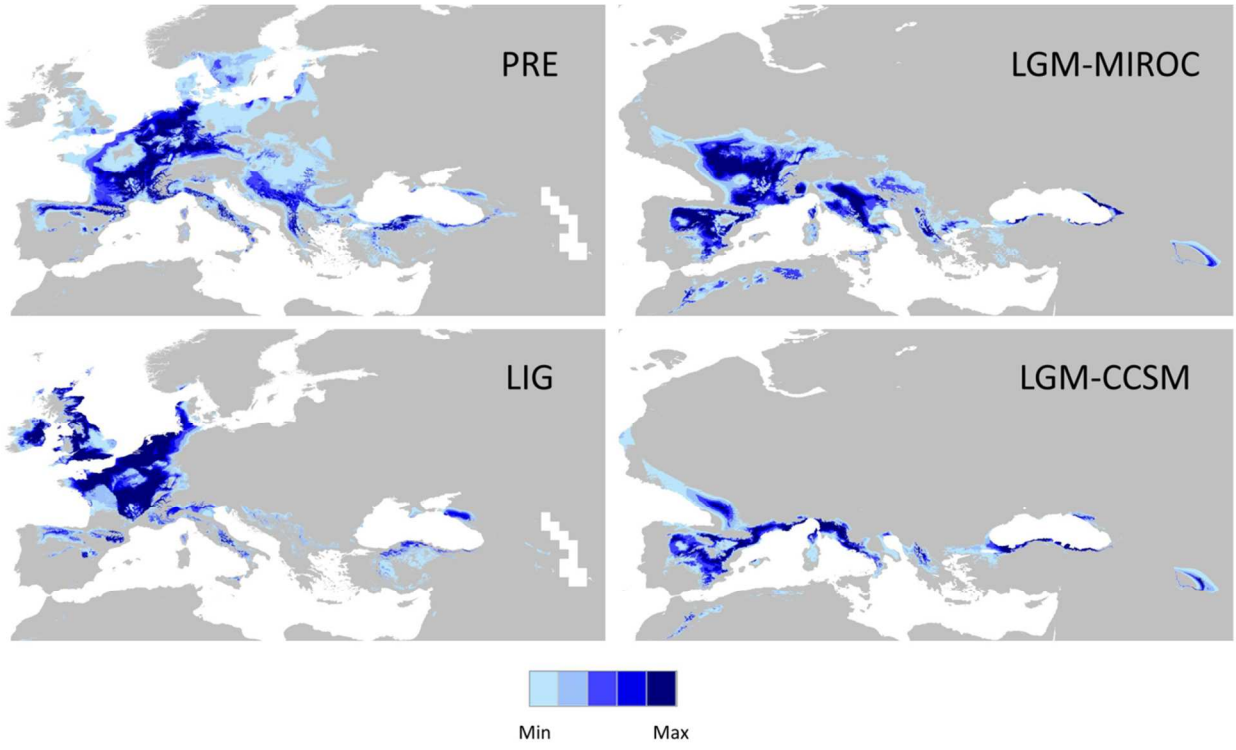

Fig. 2 BIOCLIM predicted suitability for *Taxus baccata* based on climatic variables at three time periods: LIG=Last interglacial (~120,000-140,000 yrs BP), LGM-CCSM and LGM-MIROC=Last Glacial Maximum (~21,000 yrs BP), PRE=present conditions (~1950-2000). The models were produced separately for the *Western* (153 sampling sites) and *Eastern* (64 sampling sites) gene pools. Darker colours indicate higher probabilities of suitable climatic conditions. Not suitable areas and those with medium or low suitability values (i.e., below the 5-95th percentile interval) are indicated in grey.

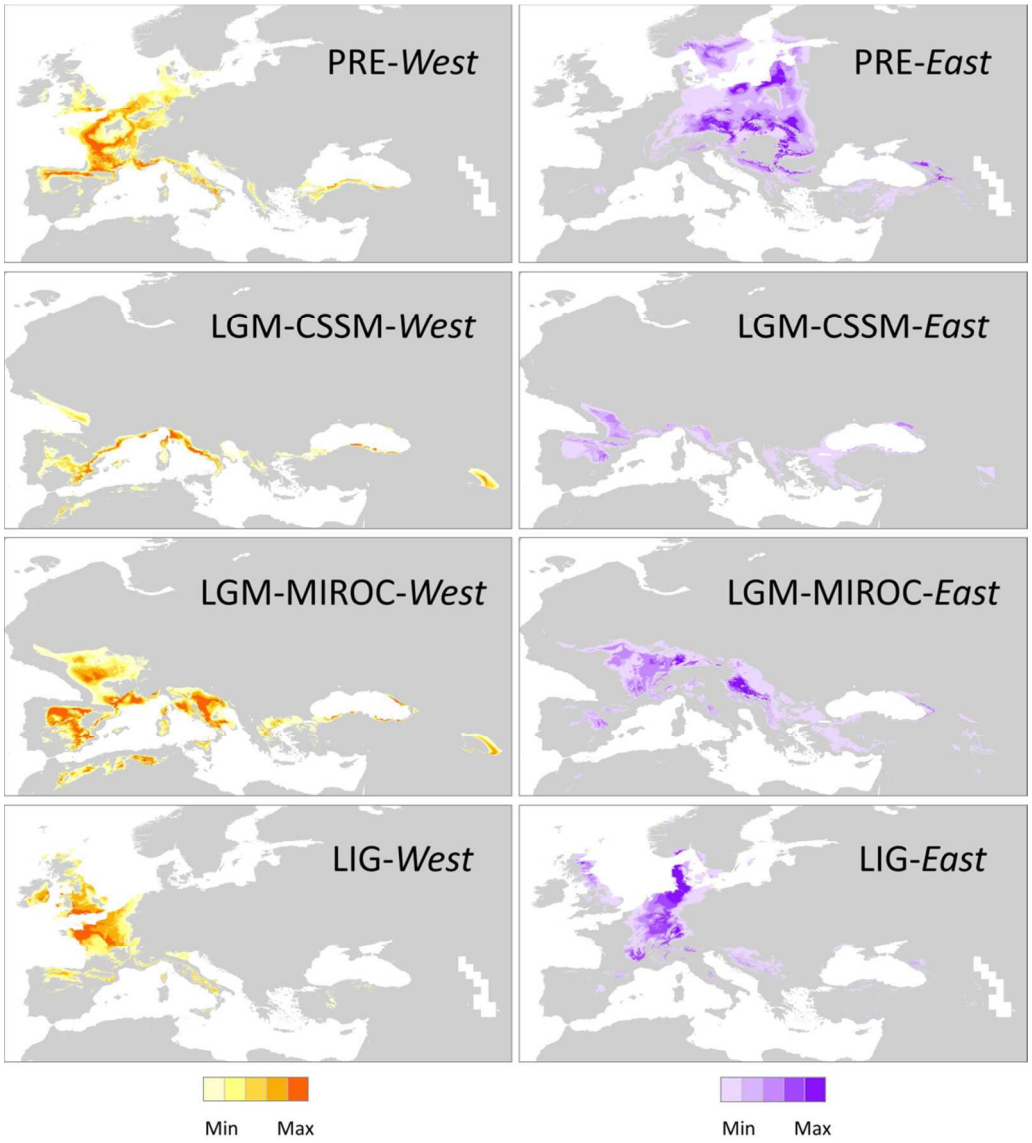

Table 1 Partial Mantel (PM) correlation (r) and Multiple Matrix Regression (MMRR) coefficients (b) between genetic distance (F_{ST}) and environmental variables for the last glacial maximum (LGM, ~21,000 yrs BP) and the last interglacial (LIG, ~120,000-140,000 yrs BP). The number of populations retained for the analyses (i.e., with suitability values of BIOCLIM predicted distributions above the 5-95th percentile intervals) are indicated in brackets behind each period considered.

	LGM-MIROC (65)			LGM-CCSM (58)			LIG (66)		
	MMRR		PM	MMRR		PM	MMRR		PM
	$b_{Geo\text{-}MIROC}$	$b_{Env\text{-}MIROC}$	$r_{Env\text{-}MIROC}$	$b_{Geo\text{-}CCSM}$	$b_{Env\text{-}CCSM}$	$r_{Env\text{-}CCSM}$	$b_{Geo\text{-}LIG}$	$b_{Env\text{-}LIG}$	$r_{Env\text{-}LIG}$
F_{ST} ~ PC1/Geo	0.151*	0.029ns	0.030ns	0.195*	-0.158*	-0.156ns	0.195***	0.110*	0.102ns
F_{ST} ~ PC2/Geo	0.147*	0.060ns	0.060ns	0.183*	-0.171*	-0.174ns	0.214***	-0.000ns	-0.000ns
F_{ST} ~ BIO1/Geo	0.131*	0.112*	0.112ns	0.176*	-0.033ns	-0.033ns	0.214***	-0.051ns	-0.050ns
F_{ST} ~ BIO2/Geo	0.155*	-0.013ns	-0.013ns	0.163*	0.061ns	0.061ns	0.194***	**0.121***	**0.123***
F_{ST} ~ BIO4/Geo	0.153*	0.001ns	0.001ns	0.179*	-0.027ns	-0.028ns	0.269***	-0.138*	-0.130ns
F_{ST} ~ BIO6/Geo	0.115*	0.144*	0.141ns	0.174*	0.054ns	0.055ns	0.147**	**0.163****	**0.152***

Variables accounting for PC1 were BIO1, BIO5, BIO6, BIO9, BIO10, B11 for LGM-MIROC, BIO1, BIO2, BIO5, BIO6, BIO8, BIO9, BIO10, B11 for LGM-CCSM, and BIO1, BIO2, BIO4, BIO6, BIO9, B11, BIO18 for LIG. Variables accounting for PC2 were the same for all periods considered, and the same as for PRE (BIO12, BIO13, BIO16, BIO19; Table S4). BIO1=Annual mean temperature. BIO2= Mean diurnal range (mean of monthly (max temp - min temp)). BIO4=Temperature seasonality. BIO6=Min temperature of the coldest month.

*** $P < 0.001$, ** $P < 0.01$, * $P < 0.05$, ns=not significant.
Positive significant tests for both Multiple Matrix Regressions and Partial Mantel tests are in bold.

References

Cornuet JM, Ravigné V, Estoup A. 2010. Inference on population history and model checking using DNA sequence and microsatellite data with the software DIYABC (v1.0). *BMC Bioinformatics* **11:** 401.

Schirone B, Caetano-Ferreira R, Vessella F, Schirone A, Piredda R, Simeone MC. 2010. *Taxus baccata* in the Azores: a relict form at risk of imminent extinction. *Biodiversity and Conservation* **19:** 1547-1565.

Shah A, Li D-Z, Möller M, Gao L-M, Hollingsworth ML, Gibby M. 2008. Delimitation of *Taxus fuana* Nan Li & R.R. Mill (Taxaceae) based on morphological and molecular data. *Taxon* **57:** 211-222.